Transactions of the Korean Nuclear Society Autumn Meeting
Gyeongju, Korea, October 26-27, 2017

Irradiation effects in Ti-added Reduced Activation Ferritic-Martensitic Steels

Jungwoo Huh[a], Chansun Shin[a*], Hyung-Ha Jin[b], Chang-hoon Lee[c]
[a]*Department of Materials Science and Engineering, Myongji University*
[b]*Nuclear Materials Safety Research Division, Korea Atomic Energy Research Institute(KAERI)*
[c]*Ferrous Alloy Department, Korea Institute of Materials Science(KIMS)*
[*]*Corresponding author: c.shin@mju.ac.kr*

1. Introduction

The Reduced Activation Ferritic / Martensitic (RAFM) steels are candidate materials for the blanket in a nuclear fusion reactor. The material will be exposed to harsh irradiation environment, hence, required to have irradiation resistance. In this study, we characterized and compared the irradiation hardening and swelling of Eurofer97 and (E97+Ti) steel. (E97+Ti) steel is a new RAFM steel developed at Korea Institute of Materials Science). The material includes titanium, which makes (Ti, W)C precipitates and refined $M_{23}C_6$ particles during tempering process. It is known that refined $M_{23}C_6$ particles contribute to increase fracture toughness by decreasing the initiation of crack, and MC-type carbides contribute to increase of the mechanical strength by blocking dislocation motion [1]. Irradiation hardening and swelling are characterized by using ion irradiation [2-4] and He irradiation, respectively.

2. Experimental

2.1 Material

The composition of (E97+Ti) steel is Fe-9wt% Cr-0.9wt% C-1wt% W-0.5wt% Ti-0.4wt% Mn-0.2wt% V-0.1wt% Ta. The steel was normalized at 1000°C for 30 minutes and tempered at temperatures of 650°C.

2.2 Self-ion irradiation and the fabrication of irradiated and non-irradiated micro-pillars

Eurofer97 and (E97+Ti)-T650 RAFM steel had been irradiated by 6.4 MeV Fe^{3+} ions at the DuET (Dual-Beam Facility for Energy Science and Technology) facility in Kyoto University. The irradiations have been performed at the temperature of 325 °C. Current density of the ion irradiation was 2.0 nA/mm^2, and total fluence was 6 x 10^{15} cm^{-2}. The depth profiles of dpa and implanted Fe-ion concentration are presented in Fig 1. The SRIM code was used to calculate the damage distribution [5]. The specimens are exposed to about 5.8 dpa and concentrations of 1450 appm at the peak locations.

As shown in Fig. 1 (top), we used cross-section polishing at the side of the irradiated samples. Micro-pillars were fabricated at the uniformly irradiated zone by using FIB (Focused Ion Beam - Helios Nanolab 450 F1) facility. Non-irradiated micro-pillars were fabricated at the location at least 30μm-away from the free surface of the samples. The fabricated micro-pillars were compressed by using UNHT (Nanoindenter - Anton Paar GmbH) for characterizing irradiation hardening [6].

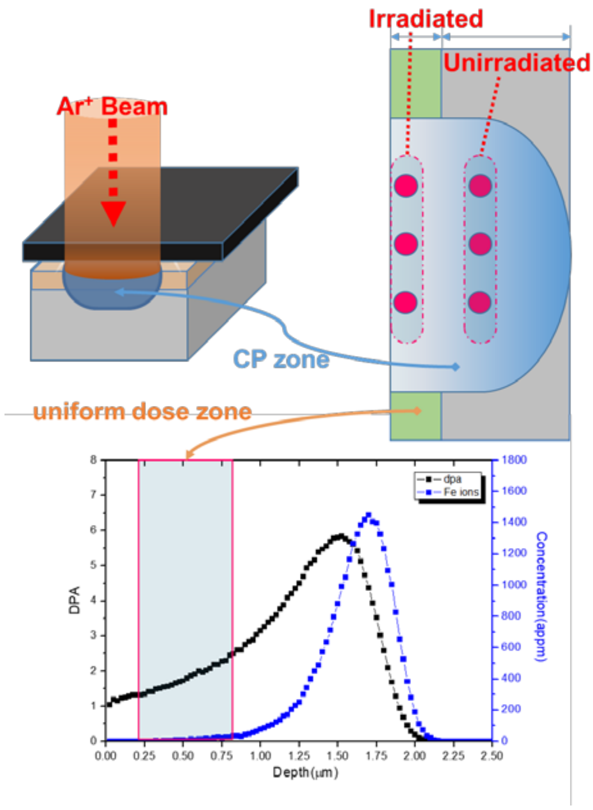

Fig. 1. The depth-DPA profile and schematic diagrams of micro-pillar location on irradiated and non-irradiated region

2.3 He ion irradiation for characterizing swelling

The specimens of Eurofer-97 and (E97+Ti)-T650 were prepared as shown in Fig. 2. A TEM grid was placed on the surface of each specimen in order to provide for He irradiation. The surface steps formed by swelling due to He irradiation are expected to be detected from He-irradiated holes and the screened area by the TEM grid. The specimens were He-irradiated at the KOMAC (Korea Multi-purpose Accelerator Complex) facility in Gyeongju, South Korea. The irradiation conditions are listed in Table 1.

Table 1. The condition of ion irradiation

Ion species	Energy	Fluence	Temperature
He ions	200 keV	5 x 10^{16}	R.T.

SRIM calculation showed 0.4 dpa-irradiation at 450 nm from the surface. After ion irradiation, these specimens are annealed 2 hours at 350 °C.

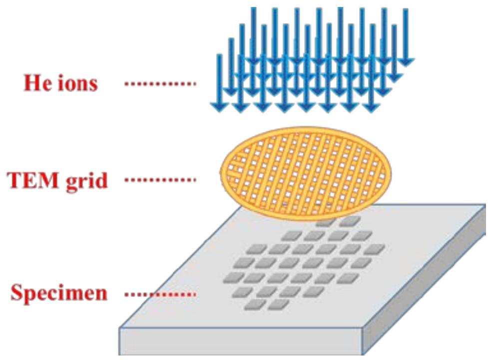

Fig. 2. Schematic design of He ion irradiation of the specimen

3. Results and discussion

Fig. 3 shows the EBSD map of the cross-section polished surface of the Eurofer97 sample. The location for the micro-pillars fabrication was carefully selected to have the same normal crystallographic orientation (marked by black and yellow arrows).

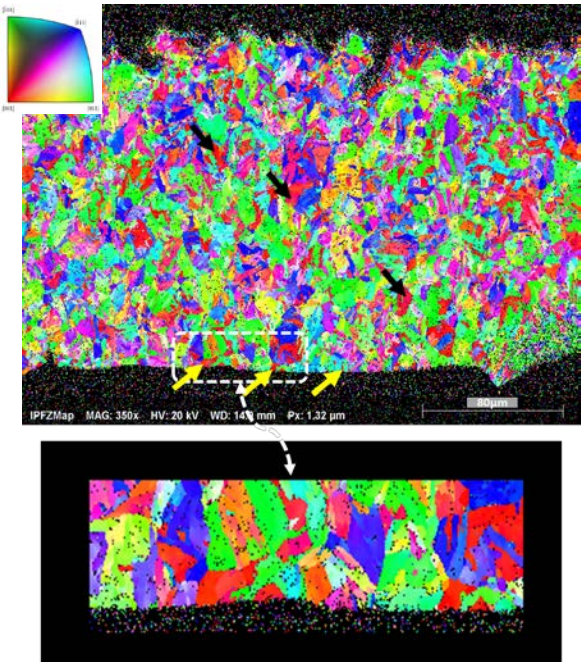

Fig. 3. EBSD map of Eurofer97. Black (yellow) arrows point the locations of non-irradiated (irradiated) micro-pillars.

Fig. 4 shows the SEM images of the micro-pillars with 500nm-diameter and 1500nm-height fabricated on the locations marked by arrows in Fig. 3. Note that micro-pillars were successfully fabricated at the location of 500nm-away from the surface.

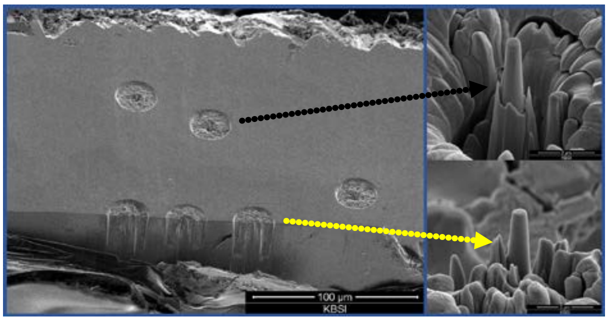

Fig. 4. SEM images of the zone of micropillar Eurofer97. Black arrows point locations of non-irradiated micropillars and yellow arrows point locations of irradiated micropillars.

The engineering stress-strain curves for irradiated and non-irradiated micro-pillars are shown in Fig. 5. The strengths of the ion irradiated micro-pillars are higher than those of the non-irradiated micro-pillars. For example, the average strengths at which the burst of slip occur are 700 MPa and 575 MPa for irradiated and non-irradiated micro-pillars, respectively. Hence, the irradiation hardening occurred. The characterization of the irradiation hardening of (E97-Ti) sample is currently underway and will be presented at the conference meeting.

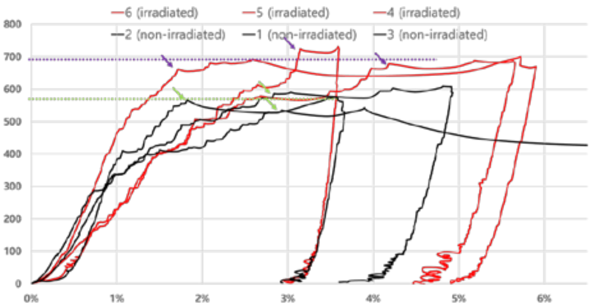

Fig. 5. The engineering stress–strain curve of Eurofer-97

The step-heights of the He-irradiated samples are shown in Fig. 6. The step-heights were measured by optical coherence tomography (NV-2700 the Surface Profiling System, Nanosystem cooperation) [7]. The measured height difference between He-irradiated and blocked regions is about 20 nm for Eurofer97 and about 15 nm for (E97-Ti). Hence, (E97-Ti) is found to be more resistant in swelling than Eurofer97. This is due to the increased interfaces of precipitate and matrix in E97-Ti.

Fig. 7 (a) shows the cross-section image of He bubble distribution in the He-implanted RAFM steel TEM lamella prepared by FIB milling. As is shown, the concentration of He bubbles increases with the penetration depth to a peak at a depth of around 600 nm, which is a typical distribution in ion-irradiated samples. Fig. 7 (b) shows a magnified view of He bubble distribution around a precipitate. He bubbles are trapped at the matrix-precipitate boundary. As is described in

Introduction, (E97-Ti) includes fine distribution of MC carbides and refined $M_{23}C_6$ particles. The interfaces of between these precipitate and matrix are known to act as sink sites for He and irradiation-induced point-defects [8].

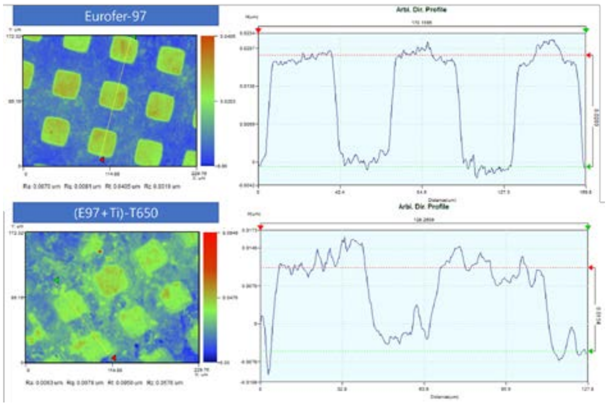

Fig. 6. Measurement the swelling effect by optical coherence tomography

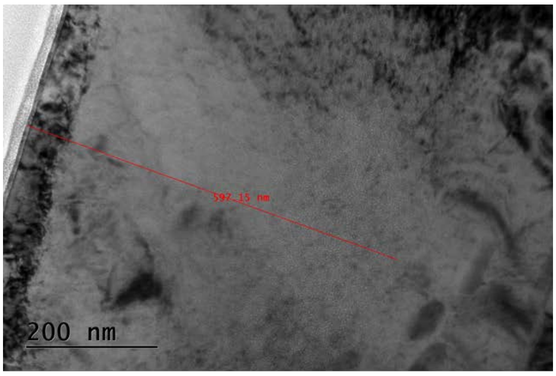

(a)

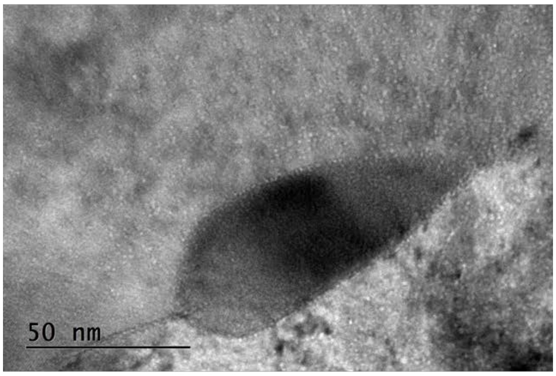

(b)

Fig. 7. TEM micrographs of He-implanted RAFM steel (a) depth-dependence of He bubble concentration, (b) He bubbles trapped around a precipitate

REFERENCES

[1] Jae Hoon Jang, Chang-Hoon Lee, Yoon-Uk Heo, Dong-Woo Suh, Stability of (Ti, M)C (M = Nb, V, Mo and W) carbide in steels using first-principles calculations, Acta Materialia, Vol.60, p. 208, 2012

[2] H. Wiedersich, J.J. Burton, J.L. Katz, Effect of mobile helium on void nucleation in materials during irradiation, Nuclear Materials, Vol.51, p. 287, 1974

[3] M. Ando a, E. Wakai, T. Sawai, H. Tanigawa, K. Furuya, S. Jitsukawa, H. Takeuchi, K. Oka, S. Ohnuki, A. Kohyama, Synergistic effect of displacement damage and helium atoms on radiation hardening in F82H at TIARA facility, Journal of Nuclear Materials, Volumes 329, p. 1137–1141, 2004

[4] S. J. Zinkle, Radiation-Induced Effects on Microstructure, Nuclear Materials, Volumes 1, Pages 65-98, S.J. Zinkle, 2012

[5] J.F. Ziegler, M.D. Ziegler, J.P. Biersack, SRIM – The stopping and range of ions in matter, Nuclear Instruments and Methods in Physics Research Section B: Beam Interactions with Materials and Atoms, Vol.268, p. 1703, 2010

[6] W.C. Oliver, G.M. Pharr, Improved technique for determining hardness and elastic modulus using load and displacement sensing indentation experiments. Journal of Nuclear Materials. Res. 7, 1564–1583, 1992.

[7] A.F. Fercher, W. Drexler, C.K. Hitzenberger, T. Lasser, Optical coherence tomography—principles and applications, Reports on Progress in Physics, Vol.66, p.239-303, 2003

[8] Z. Jiao, N. Ham, G. S. Was, Microstructure of helium-implanted and proton-irradiated T91 ferritic/martensitic steel, Journal of Nuclear Materials, Vol 367, p. 440-445, 2007